



**Universitat de Lleida**

Document downloaded from:

<http://hdl.handle.net/10459.1/60523>

The final publication is available at:

<https://doi.org/10.1016/j.jterra.2017.10.005>

Copyright

cc-by-nc-nd, (c) Elsevier, 2017



Està subjecte a una llicència de [Reconeixement-NoComercial-SenseObraDerivada 4.0 de Creative Commons](https://creativecommons.org/licenses/by-nc-nd/4.0/)

# Terrain classification using ToF sensors for the enhancement of agricultural machinery traversability

Francisco Yandun Narváez<sup>a,\*</sup>, Eduard Gregorio<sup>b</sup>, Alexandre Escolà<sup>b</sup>, Joan R. Rosell-Polo<sup>b</sup>, Miguel Torres-Torriti<sup>c</sup>, Fernando Auat Cheein<sup>a</sup>

<sup>a</sup>*Electronic Engineering Department, Universidad Técnica Federico Santa María, Valparaíso, Chile*

<sup>b</sup>*Research Group on AgroICT and Precision Agriculture, Department of Agricultural and Forest Engineering, Universitat de Lleida-Agrotecnio Center, Lleida, Spain*

<sup>c</sup>*School of Electrical Engineering, Pontificia Universidad Católica de Chile, Valparaíso, Chile*

---

## Abstract

Ground properties influence various aspects of mobile machinery navigation including localization, mobility status or task execution. Excessive slipping, skidding or trapping situations can compromise the vehicle itself or other elements in the workspace. Thus, detecting the soil surface characteristics is an important issue for performing different activities in an efficient, safe and satisfactory manner. In agricultural applications, this point is specially important since activities such as seeding, fertilizing, or ploughing are carried on within off-road landscapes which contain a diversity of terrains that modify the navigation behaviour of the vehicle. Thus, the machinery requires a cognitive capability to understand the surrounding terrain type or its characteristics in order to take the proper guidance or control actions. This work is focused on the soil surface classification by implementing a visual system capable to distinguish between five usual types of off-road terrains. Computer vision and machine learning techniques are applied to characterize the texture and color of images acquired with a Microsoft Kinect V2 sensor. In a first stage, development tests showed that only infra-red and RGB streams are useful to obtain satisfactory accuracy rates (above 90%). The second stage included field trials with the sensor mounted

---

\*Corresponding author. Tel.: +56 975209248

Email address: francisco.yandun.14@sansano.usm.cl (Francisco Yandun Narváez)

on a mobile robot driving through various agricultural landscapes. These scenarios did not present illumination restrictions nor ideal driving roads; hence, conditions can resemble real agricultural operations. In such circumstances, the proposed approach showed robustness and reliability, obtaining an average of 85.20% of successful classifications when tested along 17 trials within agricultural landscapes.

*Keywords:* Agricultural robotics, terrain classification, pattern recognition.

---

## 1. Introduction

Autonomous navigation within agricultural scenarios is a particularly challenging point since they are semi-structured environments composed of human workers, animals, obstacles and rough terrain that limit the machinery mobility and constraint its movement. In order to drive along a feasible, safe and efficient path, these vehicles must be capable of being aware of their surroundings for dealing with the constant changes of such elements within the workspace. In general, this capability is related with both object recognition (to interact with the environment or to extract information from it), and the vehicle-terrain interaction. The last point is specially challenging since the diversity of soil types present in the agricultural fields makes the scenes usually consisting of low-traction, deformable and steep-hill terrains, which can quickly degenerate the quality of the positioning and compromise the task execution. Therefore, control and path planning strategies can be executed based on the classification and characterization of the driving terrain or its surroundings (Iagnemma and Ward, 2009). In the same way, management of machinery resources (e.g., battery or fuel) can be improved, increasing the aggregated value of the agricultural activity (Michel, 2012; Xue et al., 2012). Furthermore, the integrity of the vehicle itself can be preserved by avoiding excessive slipping, skidding or even trapping conditions.

Interpretation and characterization of the terrain surface have been studied using dynamic and descriptive methodologies. Dynamic terramechanical ap-

23 proaches are performed based on known wheel-soil models which provide infor-  
 24 mation about the tractive forces involved during the navigation (Al-Milli et al.,  
 25 2010; Taheri et al., 2015). In addition, longitudinal and lateral slip effects of such  
 26 terra-mechanical interaction can be measured (Botha and Els, 2015b,a). This  
 27 knowledge, along with the kinematic characteristics of the robot, have proven  
 28 to enhance the traversability of wheeled mobile robots, specially in Mars rovers  
 29 (Ishigami et al., 2009; Brooks and Iagnemma, 2012). In these cases, the un-  
 30 avoidable limitation regarding the lack of a priori in-situ information about the  
 31 terrain, requires the robot to drive through it first in order to obtain feedback  
 32 (in relation to terrain interaction) from proprioceptive sensors on board such as  
 33 accelerometers or encoders (Brooks and Iagnemma, 2005; Ojeda et al., 2006).  
 34 Thus, using additional sensors to explore the robot surroundings for predicting  
 35 its navigation behaviour is not plausible, specially when the vehicle is driving  
 36 through completely new scenes. Unlike these scenarios, agricultural landscapes  
 37 do not present this drawbacks, since it is possible -and in some cases necessary-  
 38 to use available a-priori information in order to anticipate the upcoming navi-  
 39 gation behaviour of the vehicle.

40 A descriptive characterization of the terrain consists in representing the most  
 41 relevant properties of the soil surface as ground planes, elevation maps or terrain  
 42 classification. The first two are plausible alternatives; however, the continuously  
 43 changing characteristics of the farming lands make these methodologies imprac-  
 44 tical in some situations (e.g., when vegetation has grown or the soil has been  
 45 ploughed). Terrain classification, on the other hand, can be performed during a  
 46 normal operation and would allow to know beforehand the upcoming terrain and  
 47 discern whether a region is traversable or not, based on the latest information  
 48 acquired by the sensors (Ho et al., 2013; Ball et al., 2016).

49 Various challenging points arise when using exteroceptive and proprioceptive  
 50 information for these purposes. For example, the ambient conditions of field  
 51 operations (e.g., weather conditions or vibration) can often limit the measure-  
 52 ment capabilities. The computational cost and processing capabilities have to  
 53 guarantee practical applications. Another important point to concern is the to-



tal cost of the solution since agricultural applications like autonomous wheeled machinery are aimed to be commercially adopted by farmers. From this point of view, a trade-off between robustness and cost should be achieved to develop applications that would impact in the agricultural industry.

Given the previous context, this research work is focused on the use of a low cost sensor to obtain a descriptive interpretation of the terrain. A study and application of a classification system capable of determining the type of soil surface in front of a vehicle navigating on agricultural landscapes is proposed. Infra-red, color and depth streams are acquired with the sensor and used in a supervised classification scheme. It is shown that only infra-red information complemented with color is required to obtain high accuracy classification rates in real-time during field operations. The proposed system is tested using a mobile robot driving through a variety of agricultural terrains. It is noteworthy that this research work is not intended to determine terramechanic variables of the terrain, but to provide a complementary system that used together with those that employ wheel-ground models (Ishigami et al., 2009; Gao et al., 2013) could enhance the traversability assessment capabilities of an autonomous mobile robot.

This brief is organized as follows: Section 2 presents a review of the state of the art regarding terrain classification for diverse applications. Section 3 describes the hardware employed, as well as the methodology developed in this work. In Section 4, the experimental results, consisting of a validation and real condition tests, are shown. In Section 5 we provide the analysis and discussion of the results obtained, specially for the real condition tests. Finally, in Section 6 we present the conclusions of our work.

## 2. Related Work

Terrain characteristics influence directly in the navigation performance of wheeled mobile robots, specially in off-road scenarios like the agricultural landscapes (Prado et al., 2016). In this sense, it is reported the use of a variety of

sensors, models and processing algorithms to provide a descriptive interpretation of the soil surface. Proprioceptive information obtained with inertial and vibration sensors have been used in various studies to distinguish between several types of terrain (Brooks and Iagnemma, 2012; Park et al., 2012). However, these approaches require the vehicle to drive through the terrain first to obtain a label, which make them impractical in various situations (e.g., driving over excessively muddy soil can result in a trapping situation). To overcome this drawback, exteroceptive sensors (or a combination with proprioceptive sensors) have been employed with promising results. Specially, the robustness and working versatility in field conditions of light detection and ranging (LiDAR) or radar have made these devices commonly used (Reina et al., 2012; Fernandez, 2010). Furthermore, the first winner of the Defense Advanced Research Projects Agency (DARPA) challenge (Thrun et al., 2006) used several 2D LiDARs in a fusion scheme to classify terrain in front of the robot as occupied, free and unknown. The resulting map, along with the other systems of the robot, allowed it to autonomously drive more than 6 hours through the Mojave desert in the United States. Despite of the results reached with such range sensors, they have shortcomings that make them not suitable in certain cases that include presence of fog, excessive dust, smoke, or specular properties of the surfaces. Further, a “finer” classification of the terrain in various categories is difficult to obtain, as reported by Andújar et al. (2013).

Vision sensors have also been widely used in this context. From the color or spectral information provided by these devices, parameters such as textural or geometrical features can be obtained. For example, Ono et al. (2015) distinguished various classes of traversable or non traversable regions by employing grayscale images of a camera mounted on a space rover. For agricultural purposes, the same issue has also been addressed by using single color cameras or stereo-vision systems (Manduchi et al., 2005; Ball et al., 2016). Moreover, Zou et al. (2014) compared different approaches for terrain classification from visual information. The authors extracted different texture and color descriptors of images captured from moving robots in outdoor environments. The results

114 showed that using color and texture descriptors and learning algorithms with  
 115 2420 samples provided robustness to moderate changes in illumination. Pre-  
 116 cisely, the sensitivity of these approaches to changes in lightning makes them to  
 117 require a high number of training images in order to cover the expected condi-  
 118 tions, as reported by Angelova et al. (2007). In such work, a stereo camera and  
 119 image processing techniques were used to classify 5 types of terrain based on  
 120 texture descriptors of color images. The system used a supervised learning algo-  
 121 rithm with approximately 3000 training samples, obtaining 76.4% of accuracy  
 122 but no real time operation is reported.

123 Multi-sensor approaches can overcome the individual limitations of each de-  
 124 vice, providing robust and accurate solutions in real operation conditions. For  
 125 instance, Häselich et al. (2013) used a fusion of color and three dimensional  
 126 laser information to distinguish between 5 terrain classes. Various features from  
 127 this data were calculated and subsequently applied to a probabilistic learning  
 128 approach based on Markov Random Fields (MRF). The proposed system was  
 129 tested in field with a mobile robot, obtaining accuracies greater than 95%, but  
 130 real-time operation can not be performed when employing features from the  
 131 two sensors. In addition, combination of LiDAR, stereovision, radar and ther-  
 132 mography for detecting obstacles and traversable ground was studied by Reina  
 133 et al. (2016). This work investigated diverse learning algorithms to combine  
 134 data from these sensors in an off-line processing scheme

135 The total cost of the equipment is also an important point to take into ac-  
 136 count. Thus, approaches based on non-expensive sensors have also been studied  
 137 with promising results in various agricultural applications (Rosell-Polo et al.,  
 138 2015; Xia et al., 2015). Specifically, video gaming devices have been used as  
 139 sensing systems for terrain classification, reporting promising results (Falola,  
 140 2012; Woods et al., 2015). Further, describing soil surface under 4 different  
 141 tillage operations was studied in Marinello et al. (2015) by using a Kinect V1  
 142 sensor from Microsoft Corporation. Roughness features were obtained based on  
 143 depth streams of a commercial structured-light camera. However, these type of  
 144 sensors are intended to be used indoors, since their outdoors performance seri-

ously decrease. Recently, a new version of the Kinect device based on the time of flight principle was released, providing outdoors robustness for certain applications. A previous work of the authors of this research showed the usability of such sensor for terrain classification in conditions similar to real operations (Yandun et al., 2016). Results showed high accuracy ( $> 80\%$ ), even with streams acquired in different weather conditions using a mobile setup.

Diverse algorithms and methodologies have been studied for processing data acquired with the previously discussed sensors. Image processing, probabilistic methods or supervised learning are reported to be employed in diverse works (Brotten et al., 2012; Zou et al., 2014). However, recent studies have opted for self-learning approaches that reduced or removed the need of the training stage in learning algorithms (Otsu et al., 2016; Reina et al., 2012). These techniques usually consist in implementing two classifiers, one of them is trained with few samples or unsupervised learning. The second classifier uses the outcome of the first one to continuously learn and subsequently determine the corresponding labels. Thus, the versatility of the system is increased, providing adaptability to new scenes. Nevertheless, the resulting accuracy is prone to high error when the first classifier provides misslabelings. Furthermore, the availability of plenty a priori in-situ information (specially for agricultural applications) is an important point that solutions should take advantage.

### 3. Materials and Methods

In this work, we employed the second generation of the Kinect device (Microsoft Corporation, USA). The sensor provides infra-red (IR), color and depth streams at a maximum of 30 frames per second. In order to measure infra-red reflectance and estimate depth, it uses an IR camera with  $512 \times 424$  pixel resolution. On the other hand, the color camera has a  $1920 \times 1080$  pixel resolution. Infra-red measurements are based on active sensing, whereas depth is estimated based on a time of flight principle. It basically consists in measuring the amount of light received by synchronized detectors working in a complementary mode.

174 This configuration provides increased noise rejection and better accuracy when  
 175 compared with its predecessor. In addition, the sensor has a built-in ambient  
 176 light rejection that detects if a pixel is over saturated and resets the reflectance  
 177 value measured by such pixel (Lau, 2013). These characteristics make the sens-  
 178 ing device versatile and robust enough in a variety of outdoor applications. Spe-  
 179 cially, for terrain recognition, the authors studied the suitability of using this  
 180 device to distinguish between several agricultural soil surfaces (Yandun et al.,  
 181 2016).

### 182 3.1. *Experimental Setup*

183 We used two experimental scenarios to validate and test our system: static  
 184 and real-dynamic operation. The static setup was employed to acquire the  
 185 development dataset (i.e., training and testing data to establish and evaluate  
 186 our approach). It consisted of placing the camera facing downwards to grab  
 187 fixed depth, IR and color frames. For each terrain type studied in this brief,  
 188 we collected 820 frames per class at different illumination conditions. Once  
 189 the system was tested and validated, the sensor was mounted on the mobile  
 190 robot Pioneer 3-AT from Mobile Robots Llc, in such a way that it was pointing  
 191 downwards and forward, obtaining a view of the terrain in a range of 0.15 m to  
 192 0.9 m in front of the robot, as shown in Fig.1. This range is mainly affected by  
 193 two aspects: i) the mounting of the sensor on the robot, and ii) the maximum  
 194 range of the Kinect to obtain confident measures of depth (and therefore IR  
 195 reflectance). Thus, according to the manufacturer, a maximum range of 4.5 m  
 196 in front of the robot could be covered, with the proper setup of the sensor on  
 197 the robot.

198 To test our approach in real conditions, the robot was manually driven at  
 199 maximum linear and angular speeds of 0.5 m/s and 2.44 rad/s, respectively  
 200 through various agricultural fields, acquiring and processing the IR and color  
 201 streams at a frequency of 2 Hz.



Figure 1: Experimental setup employed to test our approach using a mobile robot driving through agricultural fields.

### 202 3.2. Architecture

203 The proposed terrain classification system employed image processing tech-  
 204 niques as well as a supervised learning approach according to the layout depicted  
 205 in Fig. 2. It allowed us to distinguish five types of agricultural soil surfaces:  
 206 sand, grass, pavement, gravel and litterfall & straw- covered. These terrains can  
 207 be cataloged surfaces of soil types from I to VIII according to the classification  
 208 provided by Stolpe (2002) for the Chilean agricultural landscapes. Additionally,  
 209 it was empirically found that traction of the robot changes when driving through  
 210 each one. Thus, distinguishing between them can led to better energy manage-  
 211 ment or avoiding dangerous hidden terrain topologies (it is not possible to know  
 212 the geometry beneath litterfall or straw covered terrain) which would compro-  
 213 mise the robot integrity (Prado et al., 2016). For field tests, we used only the IR  
 214 and color streams provided by the sensor since it was experimentally found that  
 215 depth information did not contribute to increase the classification accuracy, as  
 216 will be shown later in Section 4. Therefore, only texture and predominant color

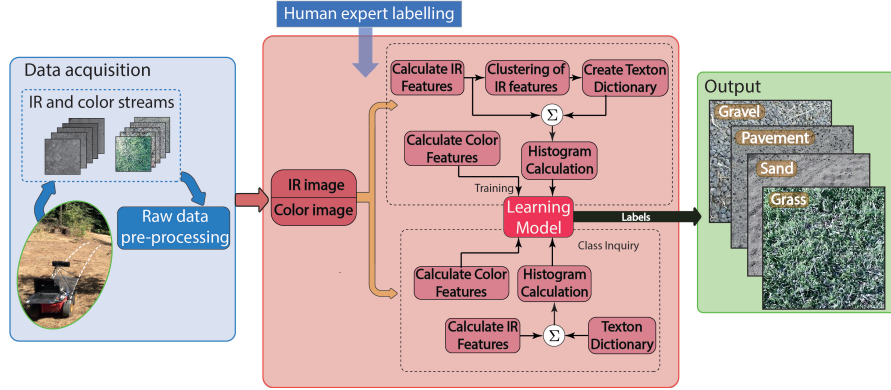


Figure 2: Block diagram of the terrain recognition system

of the terrains were analysed, setting aside its geometrical characteristics. Furthermore, our method highly relied on detecting the texture of the IR images, using color only as an additional feature to improve the classification accuracy.

The development and testing datasets were acquired at different illumination conditions and orientations, which caused various artifacts in the raw images, specially when excessive sunlight was present in the scene. To overcome this issue and to deal with the image boundary errors introduced by the sensor (Lachat et al., 2015), we cropped the raw images to retain only a central region of  $300 \times 300$  pixels. In addition, we also replaced the missing information in specific pixels with the average intensity value of its neighbours. Subsequently, texture and color features were calculated to be used as training and testing inputs in a Support Vector Machine (SVM) classifier. In this work, we employed the *one vs one* multi-class approach of this algorithm due to its balanced training characteristic and applicability for various sizes of datasets, as shown by Hsu and Lin (2002). It was also chosen to assign one label per image, since the dimensions of the space covered by each one did not allow to obtain representative patches of different terrains. Thus, the output of our system provides a single label of the terrain type in front of the robot.

It is also noteworthy that data from all sensors were synchronously acquired using an application developed in C++ and Matlab (MathWorks, USA) in a

237 shared memory framework.

### 238 3.3. *Terrain Classification*

239 As stated before, the strategy employed to visually distinguish between ter-  
240 rain types is mainly focused on the textural characterization of the images pro-  
241 vided by the sensor. As demonstrated in the authors' previous work (Yandun  
242 et al., 2016), and contrasting to the work of Angelova et al. (2007), using IR  
243 information can enhance the classification accuracy with a relative small train  
244 dataset. Further, including color or depth features along with the textural  
245 descriptors, could improve the capability of the method for detecting certain  
246 terrains. Thus, robustness in real operation conditions is also achieved, with  
247 reduced computational cost.

248 We employed the texture description methodology proposed by Varma and  
249 Zisserman (2002). It consists in building learning models based on local descrip-  
250 tors of each pixel and its statistical co-occurrence all over the image. Briefly, the  
251 most representative characteristics of the training images for each terrain class  
252 are first obtained using a clustering algorithm. Once grouped, such character-  
253 istics -called textons- represent the main descriptors of a single class. Subse-  
254 quently, textons of all training images are collected in a single texton dictionary  
255 (TD). Once it is defined, a class model per training image in form of histogram  
256 can be obtained. It is built by labelling each pixel descriptor with the position  
257 of the closest texton in the dictionary. These histograms are the feature vectors  
258 used to train a supervised classifier. In the case of the query images, the previ-  
259 ously built TD and the same methodology to obtain the histograms is applied  
260 in order to create the testing features.

261 Following this concept, various methods to obtain the local descriptors have  
262 been proposed, such as: filter responses (Varma and Zisserman, 2005), Lo-  
263 cal Binary Patterns (LBP) (Alvarez and Vanrell, 2012), Self-Invariant Feature  
264 Transform (SIFT) (Xu et al., 2012), among others. However, we employed  
265 the patch-based concept presented by Varma et al. (2009) since its results are  
266 comparable to those that apply a combination of various higher-dimensional



267 features (e.g., SIFT and its variants), as reported by Zhang et al. (2007). Thus,  
 268 the approach presented in this work arises from the idea that textures can be  
 269 considered as realizations of Markov Random Fields (MRF), as described by Li  
 270 (2009). Formally, given a rectangular region of interest (ROI)  $S$ , and a set of  $m$   
 271 random variables defined in  $S$  which can take values  $f = \{f_1, f_2, \dots, f_m\}$  (e.g.,  
 272 pixel intensities), for a MRF it can be written:

$$p(f_i | f_{S-\{i\}}) = p(f_i | f_{N_i}) \quad (1)$$

273 where  $f_i$  is the value of pixel  $i$ ,  $f_{S-\{i\}}$  represents the values of all pixels in  $S$   
 274 except  $i$ , and  $f_{N_i}$  stands for the set of pixel values in the  $N \times N$  pixel neigh-  
 275 bourhood (excluding the pixel  $i$ ). Thus, the local description of a single pixel  
 276 can be represented by the raw intensities of an  $N \times N$  square neighbourhood of  
 277 that point.

278 Thus, using this texture description methodology, we employed a  $5 \times 5$  neigh-  
 279 bourhood to obtain the local descriptors (i.e., a  $25^{th}$  dimensional vector). Then,  
 280 these vectors were clustered by using the standard K-means algorithm with  
 281  $K = 10$ , obtaining a total of 50 elements in the TD (5 classes  $\times$  10 centres).  
 282 It is noteworthy that  $K = 10$  was the value that yielded better classification  
 283 accuracy after several trials in a validation stage. Finally, the feature space is  
 284 created by 50-dimensional vectors that represent the frequency of occurrence of  
 285 each TD element in the image.

286 In parallel to the previous processing, color information was employed to  
 287 create an additional small feature vector. To this aim, the original RGB image  
 288 was first converted to the -Comission Internationale de l'Éclairage (CIE) 1976-  
 289 L\*a\*b\* colorspace (Schwiegerling, 2004). The L\* and b\* components were left  
 290 out for two reasons: i) to attenuate the effects of the lightning conditions,  
 291 and ii) it was found in the development stage that they did not contribute  
 292 to distinguish between classes. Thus, only the mean and variance values of  
 293 the a\* component were employed. In addition, the proportion of green in the  
 294 image was calculated as:  $\frac{G}{R+G+B}$ , where  $R$ ,  $G$  and  $B$  are the sum of intensity



Figure 3: Several snapshots of the robot driving through the experimental locations. Illumination varied from cloudy to clear sky conditions.

values per pixel for the R, G and B channels, respectively. When using depth streams in the validation tests, depth feature vectors consisted of four statistical measurements of roughness: mean, root mean square, skewness and kurtosis, as calculated by Marinello et al. (2015).

Finally, these descriptors (either depth or color) were aggregated to the texture feature vectors to form the input training and testing data in a multi-class Support Vector Machine classifier.

#### 4. Experimental Results

Experiments for acquiring the development dataset and subsequently run the trials with the robot were performed in three locations: i) the Botanical Garden of Viña del Mar, located at  $-33.048093^\circ$  latitude and  $-71.500135^\circ$  longitude; ii) the Sporting Club of Valparaíso, located at  $-33.024568^\circ$  latitude and  $-71.532815^\circ$  longitude; and iii) the Technical University Federico Santa María (UTFSM) central campus, located at  $-33.034796^\circ$  latitude and  $-71.595564^\circ$  longitude. All coordinates are measured using datum WGS84 as reference. These experimental locations included agricultural landscapes that together contained all the terrain types under evaluation. The trials were performed from 9 a.m. to 5 p.m. in summer and fall, obtaining shadowed and strongly illuminated scenes, as shown in Fig. 3.

The first stage of our experimental tests consisted in evaluating the classi-

315 fication performance as function of the variables given by the sensor. To this  
 316 aim, a development dataset (acquired with the static setup) consisting of 520  
 317 and 300 images for training and testing, respectively was used. This stage also  
 318 included a 10-fold cross-validation of the classification model obtained. Table 1  
 319 shows the performance of the proposed approach for different combinations of  
 320 IR, color and depth streams, along with the features employed for each case.  
 321 As can be noted, IR and color streams yielded the best results, whereas depth  
 322 information did not contribute to improve the classification rates.

Table 1: Comparison of classification accuracy rates when employing different sensor streams to characterize the terrains.

Characteristic	Features	Accuracy (%)
Infra-red	Texture description	92.57
Colour	Texture description of grayscale image	81.20
Depth	Texture description	34.61
Infra-red + color	Texture description of IR image + color features	95.40
Infra-red + depth	Texture description of IR image + depth features	89.13
Color + depth	Texture description of grayscale image + depth features	80.61
Infra-red + color + depth	Texture description of IR image + color features + depth features	91.04

323 In addition, Figure 4 shows the confusion matrix for the best validation case.  
 324 The far right column shows the accuracy for the output terrain types, whereas  
 325 the row at the bottom shows the accuracy for each true class. Finally, the cell  
 326 at the right bottom shows the overall accuracy of the classification. The most  
 327 *conflictual* terrains were sand and pavement since some images from pavement  
 328 were very similar to sand, specially from the color point of view. However, the  
 329 general performance of the proposed approach was accurate enough to test it  
 330 under real conditions.

331 Once the proposed methodology was validated, we ran a total of 17 trials  
 332 navigating with the mobile robot through the three experimental landscapes.  
 333 We acquired in average 1000 frames in each drive of the robot which were  
 334 manually labelled to obtain the ground truth. In addition, and to provide

Output Class	Sand	285	0	0	33	5	88.2% 11.8%
	Grass	3	292	4	0	0	97.7% 2.3%
	Gravel	0	2	296	2	0	98.7% 1.3%
	Pavement	10	0	0	265	2	95.7% 4.3%
	Litterfall & Straw	2	6	0	0	293	97.3% 2.7%
		95.0% 5.0%	97.3% 2.7%	98.7% 1.3%	88.3% 11.7%	97.7% 2.3%	95.4% 4.6%
		Sand	Grass	Pavement	Gravel	Litterfall & Straw	
		Ground Truth					

Figure 4: Confusion matrix for the best validation test. Only IR and color information from the sensing device was employed, yielding satisfactory detection rates. Two terrain types are often misclassified due to its visual similarity from the color and IR images.

an illustration of the data acquired by the sensor, Fig. 5 shows a 3D-color reconstruction of partial paths followed by the robot. Part of the measurements are noisy due to sunlight incidence and vibration of the vehicle, but in general, the paths are visually well rendered.

In order to evaluate the classification performance for this case, 5 statistics including accuracy (acc), precision (prec), recall (rec), specificity (spec) and F-score (Fs), were calculated. They were calculated as described by Fawcett (2006) and are aimed to measure, in a complementary way, the quality of the true positive and true negative detections, taking into account all the classification outputs. The results in terms of these metrics, along with the distance covered for each testing trial are summarized in Table 2. As can be noted, reduced performance is exhibited for some trials. A deeper analysis of the images in each one showed important variation in true positive and false negative detection rates for the reasons discussed in Section 5. However, in general, the proposed methodology to classify terrain types based only on their appearance, with data

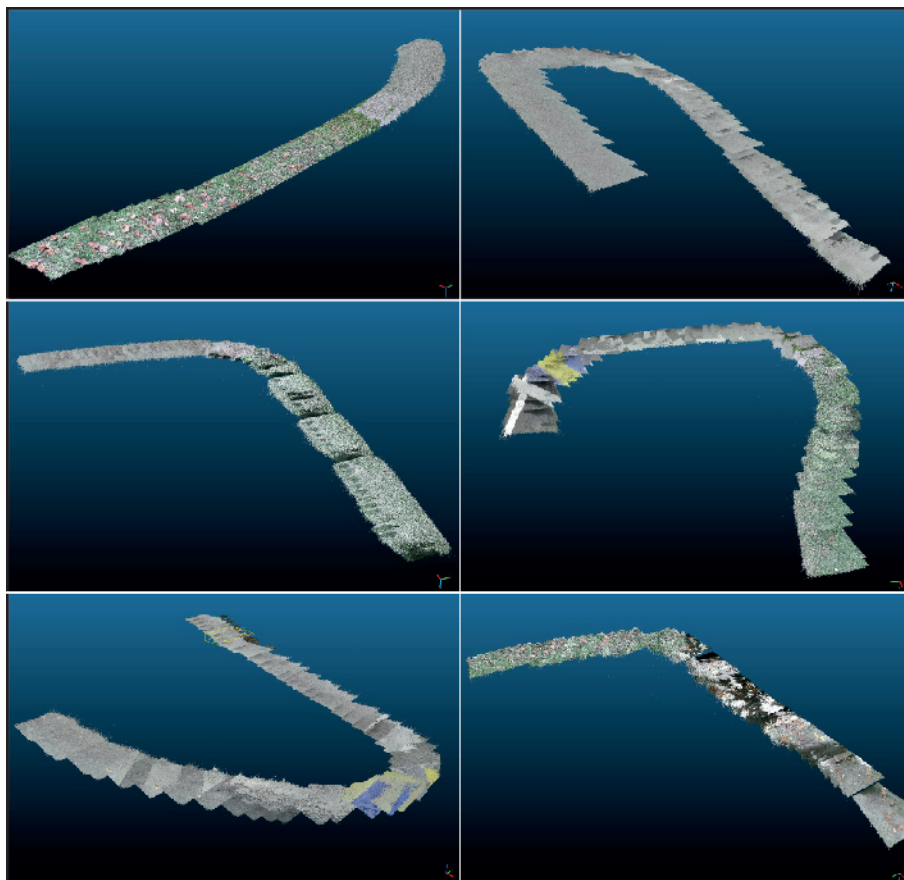


Figure 5: Three dimensional reconstructions of partial paths followed by the robot in different testing locations. The robot was manually driven on different roads in order to cover all the terrain classes classified in this work. In addition, the sensing device showed robustness when working outdoors, which allowed the scenes to be properly rendered.

acquired by a low cost sensor showed potential, even in presence of changing illumination and real driving conditions.

Table 2: Performance statistics for experiments conducted with the robot in real working conditions. A total of 17 trials were run within the three experimental locations, obtaining an overall of 15836 images.

Trial	Accuracy	Precision	Recall	Specificity	F-score	Distance(m)
1	0.80	0.80	0.80	0.95	0.80	144.63
2	0.76	0.76	0.76	0.92	0.76	121.46
3	0.77	0.77	0.77	0.94	0.77	87.63
4	0.80	0.80	0.80	0.93	0.80	173.57
5	0.91	0.91	0.91	0.98	0.91	325.70
6	0.92	0.92	0.92	0.98	0.92	124.93
7	0.72	0.72	0.72	0.91	0.72	98.69
8	0.86	0.86	0.86	0.97	0.86	119.3
9	0.92	0.92	0.92	0.98	0.92	132.31
10	0.96	0.96	0.96	0.98	0.96	107.80
11	0.79	0.79	0.79	0.95	0.79	163.00
12	0.87	0.87	0.87	0.97	0.87	168.22
13	0.82	0.82	0.82	0.95	0.82	136.11
14	0.98	0.98	0.98	0.98	0.98	286.40
15	0.73	0.73	0.73	0.91	0.73	146.46
16	0.87	0.87	0.87	0.96	0.87	424.95
17	0.82	0.82	0.82	0.95	0.82	477.05
mean	0.83	0.83	0.83	0.95	0.83	Total Distance: 3238.21 m

In addition to the previous results, Fig. 6 shows a confusion matrix that summarizes the outcomes obtained for all trials. In general, the proposed approach is able to achieve an accuracy of 83.00%, with reduced false positive and false negative detections for various terrain types in the field. However, the interclass similarity problem for pavement and sand observed in the validation stage is also exhibited in this case. Furthermore, sand and litterfall & straw also present this problem, which was not perceived in the validation stage. A close look into the images of these terrain types showed that some sandy locations were visually similar to litterfall & straw. Moreover, the most important reason for this outcome is the excessive black pixels with null information obtained in

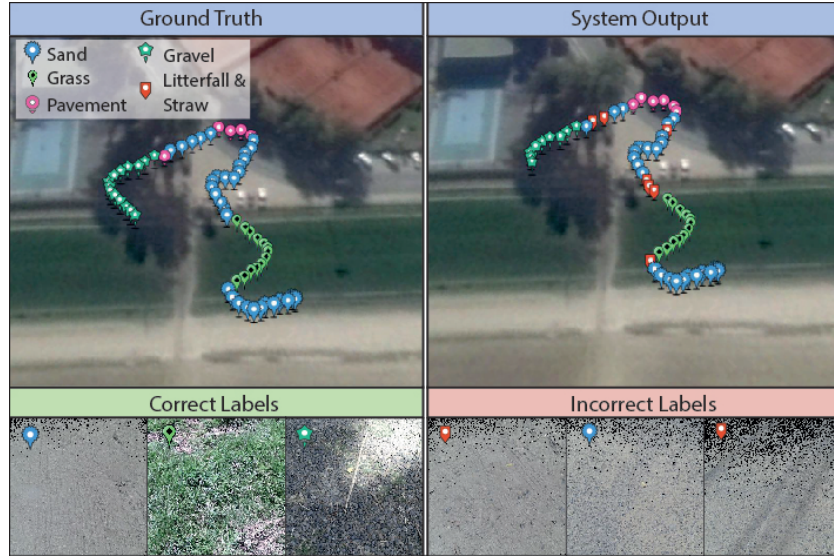
362 numerous images, as will be discussed in Section 5. Despite of these issues, the  
 363 overall performance of the proposed terrain classification system can be consid-  
 364 ered satisfactory, given the testing conditions and the low cost sensing hardware  
 365 employed.

Output Class	Sand	6876	36	0	521	245	89.6% 10.4%
	Grass	29	2788	1	2	45	97.3% 2.7%
	Gravel	22	6	743	16	23	91.7% 8.3%
	Pavement	454	4	14	1308	10	73.1% 26.9%
	Litterfall & Straw	595	98	177	50	1773	65.8% 34.2%
		86.2% 13.8%	95.1% 4.9%	79.5% 20.5%	69.0% 31.0%	84.6% 15.4%	85.2% 14.8%
		Ground Truth					
		Sand	Grass	Pavement	Gravel	Litterfall & Straw	

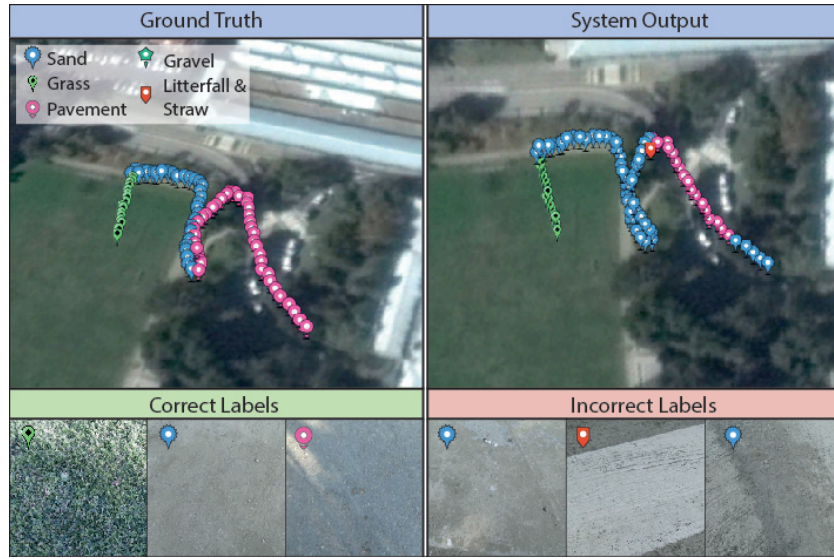
Figure 6: Confusion matrix that summarizes the overall performance of the proposed terrain classification methodology. It includes results of all tests (15836 images) conducted with the mobile robot through diverse agricultural scenes. Interclass visual similarity tends to decrease the classification performance, but in general, the terrains are correctly identified.

366 In order to illustrate the path followed by the robot, along with the labels  
 367 obtained from the proposed approach, Fig 7a and Fig. 7b show a georeferenced  
 368 and subsampled outcome for specific trials ran in two locations. They corre-  
 369 spond to 65 labels from trials 6 and 15 which originally contained 647 and 870  
 370 frames, respectively.

371 All the experiments employed an on-board computer with a 2.20 Ghz Core  
 372 i5 processor and 4 GB of RAM. With these characteristics, the processing time  
 373 in average was 14.83 min per class for the training stage (with the extended  
 374 dataset) and 0.51 s per image in the labelling stage. Since training the algorithm  
 375 can be done offline before operating in field, and considering that the labelling



(a)



(b)

Figure 7: Georeferenced and subsampled outcome of the terrain classification system for two trials. The bottom row shows RGB images of the terrain captured by the sensing device, along with coloured markers representing the output of our classification system. The ground truth for these images are (from left to right): (a) sand, grass, gravel, sand, pavement, sand; and (b) grass, sand, pavement, pavement, pavement and pavement.



time is acceptable for vehicle moving at low speeds, the proposed approach is valid from the computational effort point of view. In addition, the memory required to store the learned model, as well as the texton dictionary is only 2 Mb, which would be important when employing low-performance computers with limited storage memory.

## 5. Discussion

Validation and real operation test results demonstrated the feasibility of the approach presented to classify different types of terrains. When comparing the suitability of the streams provided by the sensor, depth information tended to decrease the classification accuracy. According to the authors, this outcome is a result of two main reasons: the sensor resolution and the redundancy introduced due to the depth measuring methodology. The former causes terrains with slight changes in depth to look similar from the sensor point of view. The latter lies in the addition of extra processing of data from the same source, since depth is measured based on the IR reflectance received by the sensor. Thus, the best results in terms of classification accuracy were obtained when employing only the IR and color streams. With this regard, the confusion matrix depicted in Fig. 4, shows that sand and pavement classes are prone to missclassifications. This issue is due to the visual similarity between these two terrains which in some cases caused confusions even for the human labeller.

The visual interclass similarity issue identified in the validation stage was confirmed in the real testing stage. In this case, the problem was more evident and spread to other terrain types. For example, some sand images were confused with litterfall & straw since both were very similar from the IR texture and color point of view. Another minor issue that also contributed to reduce the true positive and true negative rates was related to the excessive artifacts in some images due to the robot motion and the presence of objects in the soil surface that modified the appearance of the captures. In order to illustrate these problems, Fig. 8 shows color images along with its IR frames of the two

405 issues previously described. The first and second columns of the image show  
 406 pairs of highly similar color and IR images despite of their belonging to different  
 407 classes. The third and fourth columns show the excessive artifacts introduced in  
 408 some images that result in bad labelling. Most of these images in the field tests  
 409 correspond to sandy terrain, that made the algorithm to classify it as litterfall  
 410 & straw. This explains the outcome of the confusion matrix for this case (see  
 411 Fig. 6), in which sand was missclassified as litterfall & straw 595 times.

412 In contrast to the previous concerns, most of the color and IR information  
 413 acquired with the sensor allowed satisfactory results. Considering that we are  
 414 employing only 520 training samples per class, the system showed robustness in  
 415 different agricultural scenarios and testing conditions. Figure 9 shows various  
 416 challenging captures that were correctly classified despite of having shadows  
 417 and high illumination. It can be noted that color images are affected by these  
 418 problems, but the IR streams are insensitive to them.

419 The points that we have identified to reduce the classification performance  
 420 are related to the visual essence of our approach. Thus, improving the efficiency  
 421 of the current approach seems suitable by using multi-sensor fusion. In this way,  
 422 using the data acquired with an inertial sensor in a complementary way seems  
 423 plausible. The output of our system can provide “a priori” information to be  
 424 subsequently corroborated or corrected by the inertial measurements. In this  
 425 case, the robustness under sunlight and the low cost of the proposed method-  
 426 ology could offer an increased versatility which would favour its commercial  
 427 adoption.

428 Another important point of the presented work is the computational effort  
 429 (0.51s for the labelling stage). For the trials with the robot operating at the  
 430 reported linear and angular speeds, and taking into account the area in front of  
 431 the robot covered by the sensor field of view, the processing time was satisfactory  
 432 enough for real time operations. However, for speeds higher than those reported  
 433 in this work, a lower level implementation of the proposed system is certainly  
 434 required.

435 Finally, when comparing our approach with previous works, we observed

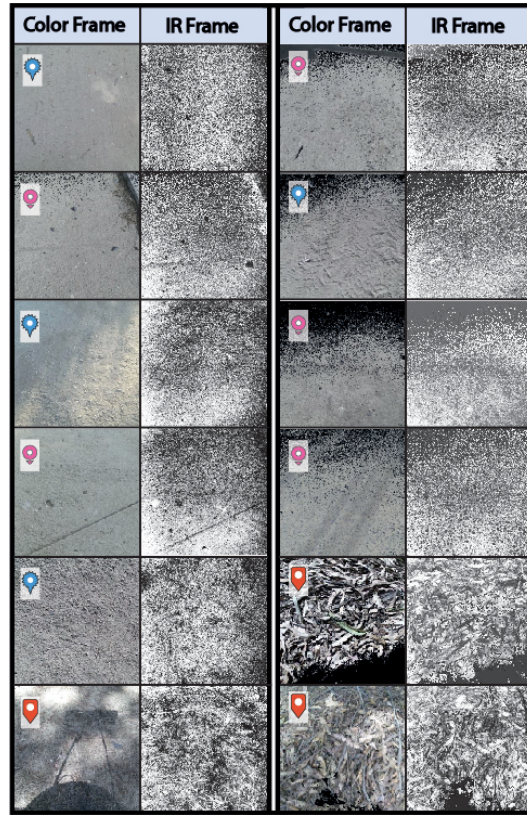


Figure 8: Examples of color images and their corresponding IR frames that show the visual similarity and excessive black pixels issues that resulted in missclassifications. The first and second columns show pairs of color and their IR images that illustrate the high similarity interclass for some captures. From top to bottom: sand, pavement, sand, pavement, sand and litterfall & straw. The third and fourth columns show pairs of color and their IR frames that illustrate the loss of information in some captures that also introduced error in the classification. The markers on each image show its true terrain type, according to the legend presented in Figure 7.

436 various pros and cons that are summarized in Table 3. Real time operation at  
437 low speeds, accuracy above 80% and low cost are the three strongest points that  
438 make the system presented in this brief comparable with those that used other  
439 sensors to the same aim: classify terrain types to analyse traversability.

Table 3: Comparison of the presented approach with others that employ different sensors and methodologies for terrain classification.

	Approach		
	Proposed Time of Flight IR description	Radar/ Laser	Stereo Vision
Pros	Requires a small dataset to be robust in changing illumination conditions.	Various works provide an statistical traversability analysis.	Can also include slip prediction.
	Reduced cost.	Large field of view.	Large field of view.
	Overall accuracy higher than 85% using more than 15 000 images (more than 3.00 km of driving).	Robust in changing illumination conditions.	A geometric description of the terrain is available.
	A geometric description of the terrain can also be obtained.		Various terrains can be detected in the same image.
Cons	Reduced field of view.	A finer classification in various terrain types can not be achieved.	Processing time is not suitable for online operation in some cases.
	Only one label is obtained per image.	Cost is high for radar and 3D laser scanners.	Sensitive to changes in illumination.
	Computation time needs to be improved.	Lack of color or spectral information.	Overall accuracy up to 76.4% using 1500 images for testing.
			Self Learning
			Do not need large training datasets.
			Are verstaile when facing new terrains
			Some works provide a statistical traversability analysis
			Rely on propiocceptive information, which limits prediction capabilities.
			Processing time is not suitable for online operation in some cases

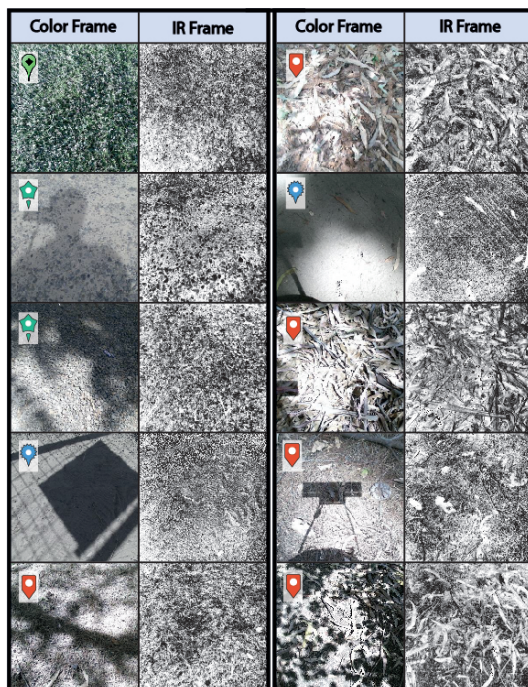


Figure 9: Examples of challenging color (1st and 3rd columns) and their IR streams (2nd and 4th columns) correctly classified by our system. These captures correspond to: grass, gravel, gravel, sand, litterfall & straw, litterfall & straw, sand, litterfall & straw, litterfall & straw and litterfall & straw, respectively. It can be noted that color frames are influenced by illumination, whereas IR frames are not, providing robustness for these conditions. The markers on each image show its true terrain type, according to the legend presented in Figure 7.

## 6. Conclusion and Further Work

This work presented the use of a visual approach to distinguish between agricultural terrains. Such information is intended to contribute to the traversability assessment of the surrounding terrain of agricultural machinery for supervision and inspection. Data acquired from a low cost sensor was used to characterize the predominant colors and texture of five representative agricultural terrain types including: sand, grass, pavement, gravel and litterfall & straw- covered. For this aim, histogram features were obtained based on exemplar local descriptors of  $5 \times 5$  neighbourhoods per pixel (called textons), obtained by means of a

449 clustering algorithm.

450     The proposed system was first validated using a static experimental setup,  
451 that allowed to identify that only the color and IR streams provided enough  
452 information to obtain satisfactory results (accuracy higher than 95%). Subse-  
453 quently, the system was tested in real working conditions by running several  
454 trials in agricultural landscapes. Mounting the sensor over the vehicle allowed  
455 to obtain an important view of its front region. However, the captured area  
456 was not enough to distinguish between representative patches of various terrain  
457 types in the same image.

458     The experimental results for the validation tests, as well as the driving ex-  
459 periments showed two main issues of the proposed approach. It was detected  
460 that acquisition glitches, along with high interclass similarity between sand and  
461 pavement reduced the accuracy and performance of our approach, specially  
462 when the sensor was mounted on the vehicle. However, in this conditions, our  
463 system is capable of obtaining an overall accuracy of 85.20%. Such outcome  
464 was considered satisfactory given the relative low number of training images  
465 and the changing illumination conditions observed during the robot navigation.  
466 Moreover, the processing time obtained in the method implementation admitted  
467 applications in real time at low speeds.

468     Given the previous discussion, the authors' further work will be focused  
469 on including other terrain types (e.g., rocky, or muddy), incorporating various  
470 sensors to enhance the classification, and implementing the proposed approach  
471 in a lower-level programming language. In addition, this work opened a new  
472 point of view to detect useful terrain characteristics for mobile robots navigation  
473 based on the spectral response (not only thermal) of the soil surface. Finally, a  
474 complete terrain characterization system would incorporate a terramechanical  
475 model of the ground-wheel interface to assess the traversability characteristics  
476 of the terrain in an integral manner.

## 477 **Acknowledgements**

478 This work was supported by the Chilean National Commission for Scien-  
479 tific and Technological Research under grant CONICYT- PCHA/Doctorado  
480 Nacional/2015-21150694, FONDECYT Grant 1171431, FB0008, DGIIP-UTFSM  
481 Chile and University of Lleida, Spain.

## 482 **References**

- 483 Al-Milli, S., Seneviratne, L.D., Althoefer, K., 2010. Track-terrain modelling  
484 and traversability prediction for tracked vehicles on soft terrain. *Journal of*  
485 *Terramechanics* 47, 151–160.
- 486 Alvarez, S., Vanrell, M., 2012. Texton theory revisited: A bag-of-words approach  
487 to combine textons. *Pattern Recognition* 45, 4315–4325. doi:10.1016/j.  
488 *patcog*.2012.04.032.
- 489 Andújar, D., Rueda-Ayala, V., Moreno, H., Rosell-Polo, J.R., Escolà, A., Valero,  
490 C., Gerhards, R., Fernández-Quintanilla, C., Dorado, J., Griepentrog, H.W.,  
491 2013. Discriminating crop, weeds and soil surface with a terrestrial LIDAR  
492 sensor. *Sensors (Basel, Switzerland)* 13, 14662–14675.
- 493 Angelova, A., Matthies, L., Helmick, D., Perona, P., 2007. Learning and Predic-  
494 tion of Slip from Visual Information. *Journal of Field Robotics* 24, 205–231.
- 495 Ball, D., Upcroft, B., Wyeth, G., Corke, P., English, A., Ross, P., Patten, T.,  
496 Fitch, R., Sukkarieh, S., Bate, A., 2016. Vision-based Obstacle Detection  
497 and Navigation for an Agricultural Robot. *Journal of Field Robotics* 33,  
498 1107–1130.
- 499 Botha, T.R., Els, P.S., 2015a. Digital image correlation techniques for measuring  
500 tyre road interface parameters: Part 2 Longitudinal tyre slip ratio measure-  
501 ment. *Journal of Terramechanics* 61, 101–112. doi:10.1016/j.*jterra*.2015.  
502 05.003.

503 Botha, T.R., Els, P.S., 2015b. Digital image correlation techniques for measuring  
504 tyre-road interface parameters: Part 1 Side-slip angle measurement on rough  
505 terrain. *Journal of Terramechanics* 61, 87–100. doi:10.1016/j.jterra.2015.  
506 04.004.

507 Brooks, C.A., Iagnemma, K., 2005. Vibration-based terrain classification for  
508 planetary exploration rovers. *IEEE Transactions on Robotics* 21, 1185–1190.

509 Brooks, C.A., Iagnemma, K., 2012. Self-Supervised Terrain Classification for  
510 Planetary Surface Exploration Rovers. *Journal of Field Robotics* 29, 445–468.

511 Broten, G., MacKay, D., Collier, J., 2012. Probabilistic obstacle detection  
512 using 2 1/2 D terrain maps, in: *Proceedings of the 2012 9th Conference*  
513 *on Computer and Robot Vision, CRV 2012*, pp. 17–23.

514 Falola, O., 2012. Drivable Region Detection for Autonomous Robots Applied to  
515 South African Underground Mining. Ph.D. thesis. University of CapeTown.

516 Fawcett, T., 2006. An introduction to ROC analysis. *Pattern Recognition*  
517 *Letters* 27, 861–874.

518 Fernandez, J.C., 2010. Characterization of Surface Roughness of Bare Agricul-  
519 tural Soils Using LIDAR. Ph.D. thesis. University of Florida.

520 Gao, H., Guo, J., Ding, L., Li, N., Liu, Z., Liu, G., Deng, Z., 2013. Longitudinal  
521 skid model for wheels of planetary exploration rovers based on terramechanics.  
522 *Journal of Terramechanics* 50, 327–343.

523 Häselich, M., Arends, M., Wojke, N., Neuhaus, F., Paulus, D., 2013. Proba-  
524 bilistic terrain classification in unstructured environments, in: *Robotics and*  
525 *Autonomous Systems*, Elsevier B.V.. pp. 1051–1059.

526 Ho, K., Peynot, T., Sukkarieh, S., 2013. A near-to-far non-parametric learn-  
527 ing approach for estimating traversability in deformable terrain, in: *IEEE*  
528 *International Conference on Intelligent Robots and Systems*, pp. 2827–2833.



529 Hsu, C.W., Lin, C.J., 2002. A Comparison of Methods for Multiclass Support  
530 Vector Machines. *IEEE Transactions on Neural Networks* 13, 415–425.

531 Iagnemma, K., Ward, C.C., 2009. Classification-based wheel slip detection and  
532 detector fusion for mobile robots on outdoor terrain. *Autonomous Robots* 26,  
533 33–46.

534 Ishigami, G., Kewlani, G., Iagnemma, K., 2009. Predictable mobility. *IEEE*  
535 *Robotics and Automation Magazine* 16, 61–70.

536 Lachat, E., Macher, H., Mittet, M.A., Landes, T., Grussenmeyer, P., 2015. First  
537 experiences with kinect V2 sensor for close range 3D modelling. *International*  
538 *Archives of the Photogrammetry, Remote Sensing and Spatial Information*  
539 *Sciences - ISPRS Archives* 40, 93–100.

540 Lau, D., 2013. The Science Behind Kinects or Kinect 1.0 versus 2.0. URL:  
541 <http://www.gamasutra.com/blogs/DanielLau/20131127/205820/>.

542 Li, S.Z., 2009. Markov Random Field Modeling in Image Analysis - Third  
543 Edition.

544 Manduchi, R., Castano, A., Talukder, A., Matthies, L., 2005. Obstacle Detec-  
545 tion and Terrain Classification for Autonomous Off-Road Navigation. *Au-*  
546 *tonomous Robots* 18, 81–102.

547 Marinello, F., Pezzuolo, A., Gasparini, F., Arvidsson, J., Sartori, L., 2015.  
548 Application of the Kinect sensor for dynamic soil surface characterization.  
549 *Precision Agriculture* 16, 601–612.

550 Michel, D.C., 2012. System of Terrain Analysis , Energy Estimation and Path  
551 Planning for Planetary Exploration by Robot Teams. Ph.D. thesis. University  
552 of Western Ontario.

553 Ojeda, L., Borenstein, J., Witus, G., Karlsen, R., 2006. Terrain Characterization  
554 and Classification with a Mobile Robot. *Journal of Field Robotics* 23, 103–  
555 122.

556 Ono, M., Fuchs, T.J., Steffy, A., Maimone, M., Yen, J., 2015. Risk-aware  
557 Planetary Rover Operation : Autonomous Terrain Classification and Path  
558 Planning, in: Aerospace Conference, pp. 1–10.

559 Otsu, K., Ono, M., Fuchs, T.J., Baldwin, I., Kubota, T., 2016. Autonomous  
560 Terrain Classification With Co- and Self-Training Approach. *IEEE Robotics  
561 and Automation Letters* 1, 814–819.

562 Park, B., Kim, J., Lee, J., 2012. Terrain Feature Extraction and Classification  
563 for Mobile Robots Utilizing Contact Sensors on Rough Terrain, in: Interna-  
564 tional Symposium on Robotics and Intelligent Sensors 2012 (IRIS 2012), pp.  
565 846–853.

566 Prado, A., Auat Cheein, F.A., Torres-Torriti, M., 2016. Probabilistic Ap-  
567 proaches for Self-tuning Path Tracking Controllers using Prior Knowledge  
568 of the Terrain, in: 2016 IEEE/RSJ International Conference on Intelligent  
569 Robots and Systems, pp. 3095–3100.

570 Reina, G., Milella, A., Rouveure, R., Nielsen, M., Worst, R., Blas, M.R., 2016.  
571 Ambient awareness for agricultural robotic vehicles. *Biosystems Engineering*  
572 146, 114–132.

573 Reina, G., Milella, A., Underwood, J., 2012. Self-learning classification of radar  
574 features for scene understanding. *Robotics and Autonomous Systems* 60,  
575 1377–1388.

576 Rosell-Polo, J.R., Auat Cheein, F., Gregorio, E., Andújar, D., Puigdomènech,  
577 L., Masip, J., Escolà, A., 2015. Advances in Structured Light Sensors Applica-  
578 tions in Precision Agriculture and Livestock Farming. *Advances in Agronomy*  
579 133, 71–112.

580 Schwiegerling, J., 2004. Field Guide to Visual and Ophthalmic Optics.

581 Stolpe, N., 2002. Clasificaciones Interpretativas. Technical Report. National  
582 Institute of Agricultural Research of Chile. URL: [http://www2.inia.cl/  
583 medios/biblioteca/serieactas/NR29051.pdf](http://www2.inia.cl/medios/biblioteca/serieactas/NR29051.pdf).

584 Taheri, S., Sandu, C., Taheri, S., Pinto, E., Gorsich, D., 2015. A technical survey  
585 on Terramechanics models for tire-terrain interaction used in modeling and  
586 simulation of wheeled vehicles. *Journal of Terramechanics* 57, 1–22.

587 Thrun, S., Montemerlo, M., Dahlkamp, H., Stavens, D., Aron, A., Diebel,  
588 J., Fong, P., Gale, J., Halpenny, M., Hoffmann, G., Lau, K., Oakley, C.,  
589 Palatucci, M., Pratt, V., Stang, P., Strohband, S., Dupont, C., Jendrossek,  
590 L.e., Koelen, C., Markey, C., Rummel, C., Niekerk, J.V., Jensen, E., Alessan-  
591 drini, P., Bradski, G., Davies, B., Ettinger, S., Kaehler, A., Nefian, A., Ma-  
592 honey, P., 2006. Stanley : The Robot that Won the DARPA Grand Challenge.  
593 *Journal of Field Robotics* 23, 661–692.

594 Varma, M., Varma, M., Zisserman, A., Zisserman, A., 2009. A Statistical Ap-  
595 proach To Material Classification Using Image Patch Exemplars. *IEEE Tran-*  
596 *sactions on Pattern Analysis and Machine Intelligence* 31, 2032–2047.

597 Varma, M., Zisserman, A., 2002. Classifying Images of Materials : Achieving  
598 Viewpoint and Illumination Independence. *Lecture notes in computer science*  
599 , 255–271.

600 Varma, M., Zisserman, A., 2005. A statistical approach to texture classification  
601 from single images. *International Journal of Computer Vision* 62, 61–81.

602 Woods, M., Guivant, J., Katupitiya, J., 2015. Terrain Classification and Seg-  
603 mentation using Non-Semantic Range Data, in: *Australasian Conference on*  
604 *Robotics and Automation (ACRA)*, Canberra.

605 Xia, C., Wang, L., Chung, B.K., Lee, J.M., 2015. In Situ 3D Segmentation of  
606 Individual Plant Leaves Using a RGB-D Camera for Agricultural Automation.  
607 *Sensors (Basel, Switzerland)* 15, 20463–79.

608 Xu, Y., Huang, S., Ji, H., Fermüller, C., 2012. Scale-space texture description  
609 on SIFT-like textons. *Computer Vision and Image Understanding* 116, 999–  
610 1013. doi:10.1016/j.cviu.2012.05.003.

- 611 Xue, J., Zhang, L., Grift, T.E., 2012. Variable field-of-view machine vision  
612 based row guidance of an agricultural robot. *Computers and Electronics in*  
613 *Agriculture* 84, 85–91.
- 614 Yandun, F., Gregorio, E., Zuñiga, M., Escolà, A., Rosell-Polo, J.R., Auat  
615 Cheein, F., 2016. Classifying Agricultural Terrain for Machinery Traversabil-  
616 ity Purposes, in: *AGRICONTROL 2016: The 5th IFAC Conference on Sens-*  
617 *ing, Control and Automation for Agriculture*, Elsevier. pp. 457–462.
- 618 Zhang, J., Marszałek, M., Lazebnik, S., Schmid, C., 2007. Local features and  
619 kernels for classification of texture and object categories: A comprehensive  
620 study. *International Journal of Computer Vision* 73, 213–238. doi:10.1007/  
621 s11263-006-9794-4, [arXiv:arXiv:1011.1669v3](#).
- 622 Zou, Y., Chen, W., Xie, L., Wu, X., 2014. Comparison of different approaches  
623 to visual terrain classification for outdoor mobile robots. *Pattern Recognition*  
624 *Letters* 38, 54–62.